The Effects of Model Resolution on the Simulation of Regional Climate Extreme Events*

TANG Jianping[1,2†](汤剑平), ZHAO Ming[1](赵 鸣), and SU Bingkai[1](苏炳凯)

1 *Key Laboratory for Mesoscale Severe Weather of Education Ministry, Department of Atmospheric Sciences, Nanjing University, Nanjing* 210093

2 *Key Laboratory of Regional Climate-Environment Research for Temperate East Asia (RCE-TEA), Chinese Academy of Sciences, Beijing* 100029

(Received March 4, 2007)

ABSTRACT

The fifth-generation Pennsylvania State University/NCAR Mesoscale Model Version 3 (MM5V3) was used to simulate extreme heavy rainfall events over the Yangtze River Basin in June 1999. The effects of model's horizontal and vertical resolution on the extreme climate events were investigated in detail. In principle, the model was able to characterize the spatial distribution of monthly heavy precipitation. The results indicated that the increase in horizontal resolution could reduce the bias of the modeled heavy rain and reasonably simulate the change of daily precipitation during the study period. A finer vertical resolution led to obviously improve rainfall simulations with smaller biases, and hence, better resolve heavy rainfall events. The increase in both horizontal and vertical resolution could produce better predictions of heavy rainfall events. Not only the rainfall simulation altered in the cases of different horizontal and vertical grid spacing, but also other meteorological fields demonstrated diverse variations in terms of resolution change in the model. An evident improvement in the simulated sea level pressure resulted from the increase of horizontal resolution, but the simulation was insensitive to vertical grid spacing. The increase in vertical resolution could enhance the simulation of surface temperature as well as atmospheric circulation at low levels, while the simulation of circulation at middle and upper levels were found to be much less dependent on changing resolution. In addition, cumulus parameterization schemes showed high sensitivity to horizontal resolution. Different convective schemes exhibited large discrepancies in rainfall simulations with regards to changing resolution. The percentage of convective precipitation in the Grell scheme increased with increasing horizontal resolution. In contrast, the Kain-Fritsch scheme caused a reduced ratio of convective precipitation to total rainfall accumulations corresponding to increasing horizontal resolution.

Key words: regional climate, resolution, extreme event, convective precipitation

1. Introduction

Since regional climate change has significant impacts on the development of economy and society, more and more countries and scientists pay increasing attention on the research of regional climate change and variability. Currently, the simulation of regional climate change mainly relies on the regional climate model (RCM), which is a high-resolution and limited-area model and is nested into the global circulation model (GCM) for simulating and predicting regional climate change. Early studies (e.g., Giorgi et al., 1993 a, b; Leung et al., 2003; Wang et al., 2004) have documented the development, state-of-the-art models, and applications of the RCM as well as the prospect of the RCM. An important objective of the developing RCM is to capture the characteristics in regional climate change using higher resolutions than the GCM. With increasing of computing resources and great demand of assessing regional climate change, the resolution of the RCM gradually increases in applications. Nowadays, the horizontal resolution of the RCM is usually about 50 km. Higher-resolution models have been investigated as well (Christensen et al., 1998; Leung et al., 2003a, b).

Increasing the resolution improves model simulations and predictions in numerical weather predications (Kalnay et al., 1998; Colle et al., 2000), because

*Supported by National Key Program for Developing Basic Sciences under No. 2006CB400500, National Natural Science Foundation of China under Grant No. 40475035, and the open research fund from the Key Laboratory of Regional Climate-Environment Research for Temperate East Asia (RCE-TEA).

†Corresponding author: jptang@nju.edu.cn.

a high-resolution model can better represent the atmospheric dynamics and mesoscale forcing, and data assimilation in the model may take in high-resolution observations. However, the impacts of the resolution on climate predictions are not conclusive and show large uncertainties. Some experiments in long-term climate modeling demonstrated a good effect of increasing resolution on the simulation of large-scale atmospheric circulation, while other studies showed a reverse effect on the GCM simulation. For example, Giorgi et al. (1994) studied the effects of different horizontal resolutions on simulating precipitation using the NCAR RegCM2 model. They found that large-scale average precipitation is extremely sensitive to the horizontal resolution, while precipitation intensity and frequency, surface sensible heat flux and latent heat flux, and water energy balance show high sensitivity to the horizontal resolution; on the other hand, the impacts of physical parameterization schemes play more important role on the precipitation simulation than changing the resolution. Zhao and Luo (1999) indicated that the precipitation distribution with a finer vertical resolution is better than that with a coarse vertical resolution for the climate simulation in East Asia, but the simulations with finer vertical resolutions tend to cause spurious extreme precipitation cells. Leung and Qian (2003) applied two nesting methods to investigate the effects of different resolutions on long-term regional climate simulation. Their studies showed that higher-resolution models improve winter precipitation simulation along coastal areas and valleys, while high-resolution modeling improves the precipitation distribution and regional averaged precipitation accumulations in summer. In a summary, increasing resolution can improve the model ability of simulating regional climate to some extent.

An effective method to assess the impacts of the resolution on climate simulation is to compare the RCM simulations at different resolutions driven by the large-scale climate model. Giorgi et al. (1994) studied regional climate simulation by changing the resolution from 200 to 50 km. Denis et al. (2002) suggested that the ratio of the resolution between the large-scale forcing model and the RCM should not surpass 12, in order to retrieve sufficient information on regional climate scales. Because the resolution of the large-scale NCEP/NCAR reanalysis data is about 250 km, it is difficult to simulate regional climate at a finer scale of 20 km or higher resolutions using the NCEP/NCAR data to drive the RCM. Most current experiments for the resolution's effects on regional climate used relatively coarse resolution (about 50 km or coarser). Some simulations applied the nesting techniques to conduct such experiments. In addition, there are limited studies about the impacts of the horizontal resolution on complex terrain and land surface processes in regional climate in East Asia. This paper adopts the higher-resolution ($1^\circ \times 1^\circ$) NCEP FNL data to drive the PSU/NCAR MM5V3 with varied resolutions (90-15 km). The impacts of the resolution on simulating extreme climate events in China are analyzed, with the emphasis on the change in precipitation and atmospheric circulation due to changing the resolution. This work may facilitate applications of the higher-resolution RCM in the future.

2. Model configuration and data

The model ability of simulating extreme events is a critical indicator of the RCM. Extreme rainfall events are one of the most severe short-term climate disasters in China, such as the tremendous loss of life and property caused by rainfall extremes over the Yangtze-Huaihe River Basin and Yangtze River Basin in 1954, 1991, 1998, and 1999. Therefore, studying the impacts of the resolution on short-term climate simulation, especially extreme climate events (such as rainfall), possesses a significant meaning.

To verify the resolution's impacts on extreme regional climate events, the PSU/NCAR MM5V3 was used in several experiments to simulate extreme rainfall events over the Yangtze River Basin in June 1999. Previous studies showed that the MM5V3 is able to perform regional climate simulation (Tang et al., 2003; Liu, 2003; Liang et al., 2001). The MM5V3 contains better physical packages, and is coupled with radiation and land surface processes that are very critical for simulating short-term climate. The physical schemes include the Grell (GR) or Kain-Fritcsh (KF) cumulus parameterization, mixed ice phase process, CCM2 radiation scheme, NOAH land surface processes, and MRF boundary layer parameterization. The study domain is centered at 30°N, 105°E, covering an area of 2700 km×2700 km (Fig.1). Initial and boundary conditions are provided by the NCEP final analyses (FNL, http://dss.ucar.edu/datasets/ds083.2). The NCEP FNL, available every 12 h, are at 1°×1° horizontal resolution and 21 vertical levels with a top pressure of 100 hPa. Weekly average sea surface temperature from the NCEP Reynolds data (Reynolds and Marsico, 1993) provided sea surface temperature in the model. Extreme rainfall events over the Yangtze-Huaihe River Basin in June 1999 were simulated by selecting several horizontal resolutions of 90, 60, 30, and 15 km and vertical resolutions of 23 and 14 sigma levels (Table 1).

The integration of the models was accomplished on the Blue-Light high-performance Linux cluster (Su et al., 2002) at the Global Change Research Center of Nanjing University.

3. Results

3.1 Precipitation

During the summer of 1999, extreme floods occurred again over the Yangtze River Basin after 1998. Since 22 June 1999, extreme rainfall events continued over 10 days over the lower Yangtze River Basin. The extreme precipitation band located at the border between Hunan and Hubei Provinces, crossed the Dabie Mountains, and extended to the Yangtze River Estuary. Over the northeastern part of the south Yangtze River Basin, total precipitation accumulations reached 300-700 mm, which was 3-4 times of the normal

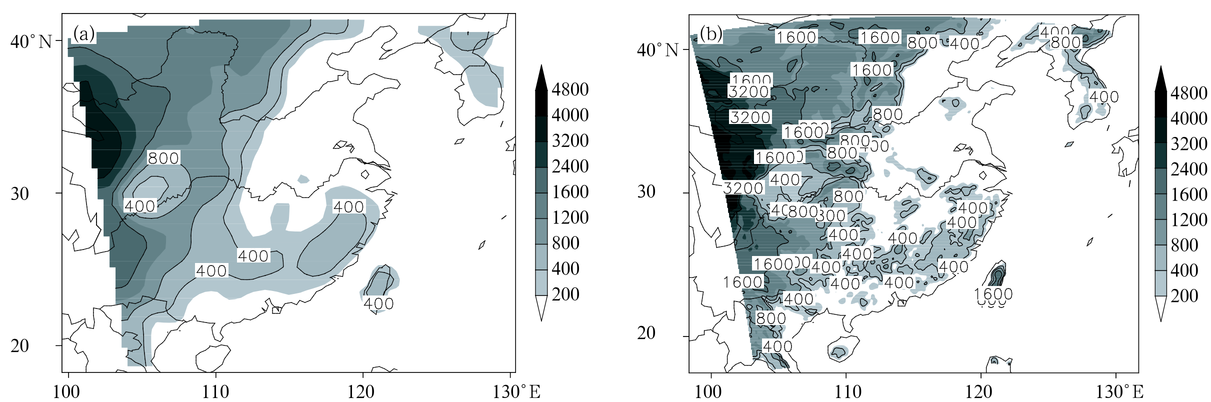

Fig.1. Model domain and topography with 90-km (a) and 15-km (b) resolutions.

Table 1. Experiments configurations with different resolutions

Experiment	Horizontal resolution	Topography resolution	Convective scheme	Vertical level
GR-90-L23	90	30′	Grell	23
GR-60-L23	60	30′	Grell	23
GR-30-L23	30	10′	Grell	23
GR-15-L23	15	5′	Grell	23
GR-90-L14	90	30′	Grell	14
GR-60-L14	60	30′	Grell	14
GR-30-L14	30	10′	Grell	14
GR-15-L14	15	5′	Grell	14
KF-90-L23	90	30′	Kain-Fritsh	23
KF-60-L23	60	30′	Kain-Fritsh	23
KF-30-L23	30	10′	Kain-Fritsh	23
KF-15-L23	15	5′	Kain-Fritsh	23
KF-90-L14	90	30′	Kain-Fritsh	14
KF-60-L14	60	30′	Kain-Fritsh	14
KF-30-L14	30	10′	Kain-Fritsh	14
KF-15-L14	15	5′	Kain-Fritsh	14

amount during the same period over the year, and average daily intensity of extreme heavy rainfall surpassed 100 mm. Precipitation amounts in many cities, such as Shanghai, Anqing, Suzhou, and Hangzhou reached the highest historical value during the same period since 1949. Severe floods and urban flood disasters happened in South Jiangsu and Anhui Provinces, North Zhejiang Province, and some parts of Shanghai City and Hubei Province, Hunan and Jiangxi Provinces as well as other regions. This caused tremendous damages to local economy and great losses of human life. Observed precipitation and surface temperature were provided by the data center of the National Meteorological Center. The precipitation data included daily precipitation accumulations over 700 ground stations. Observed total precipitation accumulations in June 1999 (Fig.2) show that an extreme heavy precipitation band with a magnitude of over 600 mm situates at the south of the middle and lower Yangtze River Basin, which extends from North Jiangxi Province, across South Anhui Province, Jiangsu Province, and to the Yangtze River Estuary. The extreme precipitation center exceeds 1000 mm in South Anhui Province.

Figure 3 shows the total precipitation over the middle and lower Yangtze River Basin in June 1999 using the Grell cumulus parameterization with different horizontal and vertical resolutions. Simulations with various horizontal and vertical resolutions provide a major precipitation band along 28°-32°N, while extreme precipitation centers and locations vary. First, precipitation accumulations with 14 vertical levels but different horizontal resolutions are plotted in the left of Fig.3. The simulation with 90-km horizontal resolution exhibits weaker intensity for extreme rainfall events over this area and a major precipitation band to the east. The 60-km runs show reasonable spatial precipitation distribution over the study period and domain, e.g., the extreme rainfall center at 600 mm is well simulated, although the intensive center in South Anhui Province slightly shifts to the east. For the 30-km runs, the distribution of the 400-mm precipitation is comparable with the observations, while the 600-mm extremes have smaller spatial extent to the south and a dominated center over the ocean east of 122°E. At 15-km resolution, the areas of 600-mm extreme precipitation are similar to the observed distribution and extreme precipitation centers are dominated in partial Anhui Province, south of the Yangtze River, while the 400-mm precipitation distribution has smaller extent. Second, the simulations with a finer vertical resolution of 23 levels (the right column in Fig.3) are compared with the simulations of 14 vertical levels. The 90-km runs with 23 vertical levels show a similar precipitation distribution as that with 14 levels, such as a heavy rainfall center over the ocean east of 122°E, but weaker precipitation amounts in Wuhan region of the middle Yangtze River Basin. At 60-km resolution, the rainfall

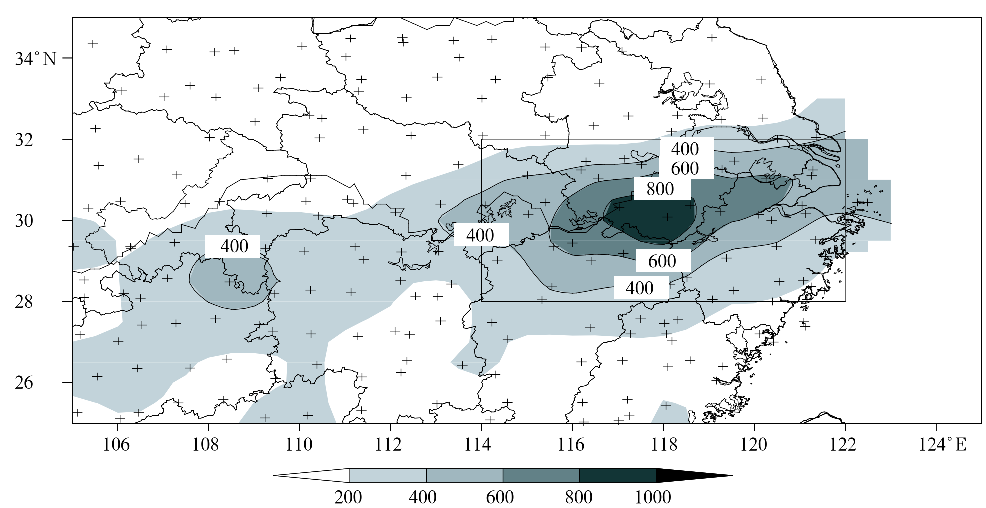

Fig.2. Observed monthly precipitation (unit: mm) in June 1999 (cross symbols: observation stations).

intensity decreases, the 400-mm precipitation region shifts northward, and the extent of the 600-mm extremes decreases with a northward shift, compared with the simulations using 14 vertical levels. Referenced to the observation, the 30-km experiments demonstrate an enlarged region exceeding 600 mm with more accurate locations of extremes, and capture the extreme center at 30°N, 116°E with a slight westward displacement. At 15-km resolution, the extent of the 400- and 600-mm precipitation thresholds is improved compared with ones using 14 vertical levels, but the intensity of the 600-mm extremes decreases and the extremes' location becomes worse. Last, the precipitation extent has not shown a consistent increase

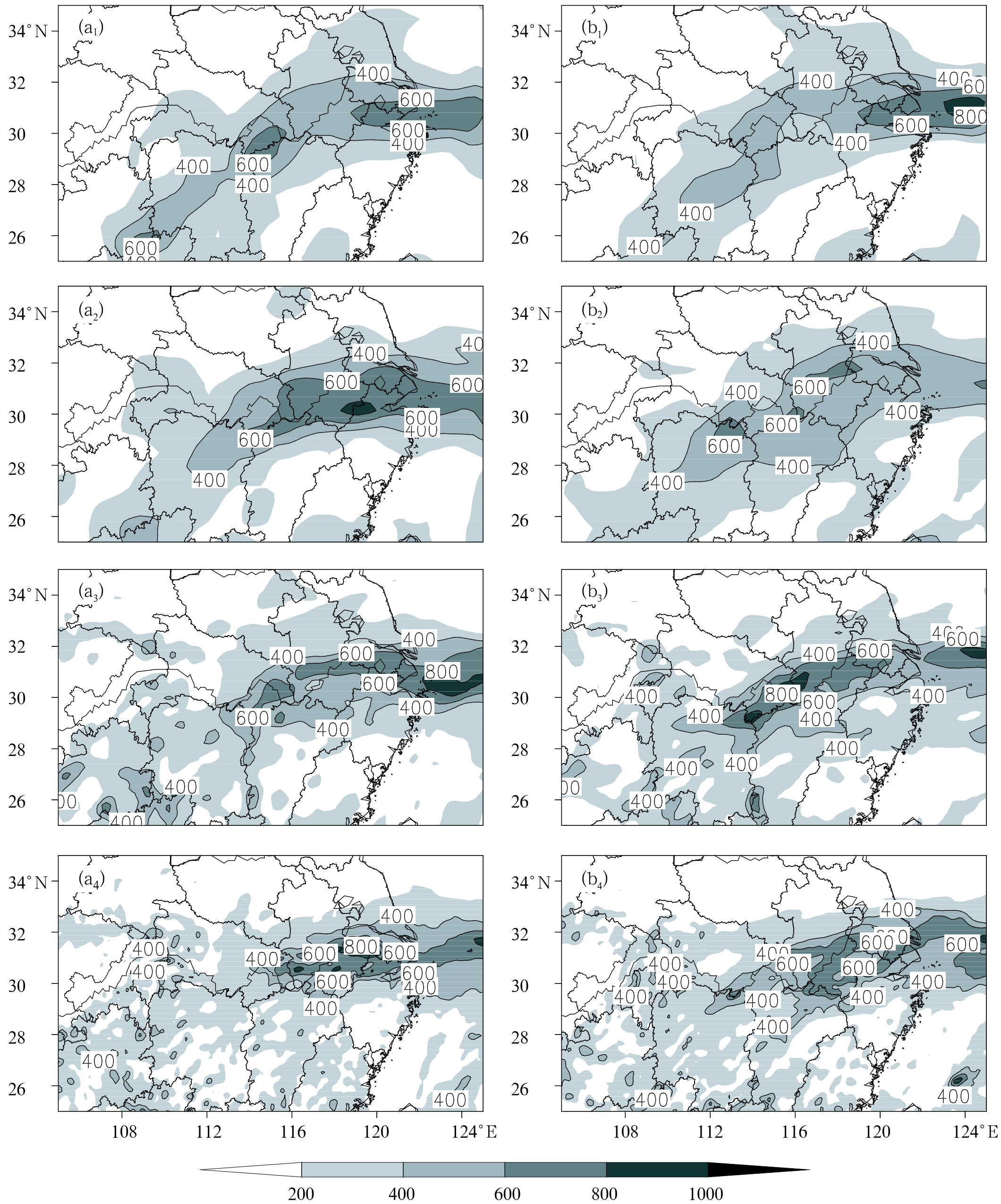

Fig.3. Simulated monthly precipitation (unit: mm) in June 1999 with different resolutions by the Grell cumulus parameterization (left column: 14 levels, and right column: 23 levels; resolutions from top to bottom: 90, 60, 30, and 15 km).

with increasing horizontal resolution, such as the 400-mm precipitation extent occasionally decreases, while the local extreme intensity generally increases. Moreover, heavy rainfall events to a small extent outside the extreme precipitation band increase, which mainly result from exemplified local effects of topography and land surface processes by increasing horizontal resolution.

To further analyze the effects of the resolution on the rainfall simulation, daily variation of precipitation (Fig.4) is computed for the extreme precipitation region (28°-32°N, 114°-122°E, the inner domain of Fig.1). The observed daily variation of precipitation shows that there are three intensive periods over the middle and lower Yangtze River Basin, i.e., 8-11, 16-18, and 22-30 June 1999. All simulations with varied horizontal and vertical resolutions are able to simulate the daily variation over this region and the three intensive periods, but with different daily intensities. Generally, the first intensive period is overestimated by all experiments, although the 15- and 30-km runs exhibit less wet biases. The second intensive period is underestimated by the experiments, except for the 15-km simulations. The third intensive period is well simulated by all experiments.

Table 2 gives the differences of the simulated and observed daily mean precipitation accumulations over the extreme region (Fig.1) during the three intensive periods in June 1999, as well as corresponding ratios

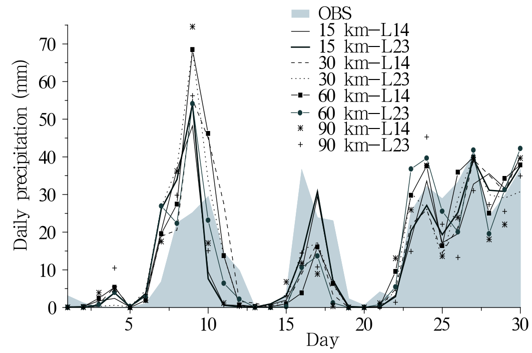

Fig.4. Observed and simulated daily variation of precipitation (unit: mm) in June 1999 for the selected domain (28°-32°N, 114°-122°E).

of the convective rainfall in the total rainfall. The GR-15-L23 (the Grell scheme, 15-km horizontal resolution and 23 vertical levels) scheme shows the smallest discrepancies between the simulations and observations for the three intensive periods. This suggests that the model ability of simulating precipitation increases with increasing resolution. The monthly precipitation resembles the observations for the GR-60-L14 scheme, however, it is caused by an overestimation of the first intensive period using this scheme that compensates the underestimation for the second and third periods. Table 2 shows improved results by increasing horizontal resolution from 90 to 15 km and increasing percentages of the convective rainfall with a higher vertical resolution.

Table 2. The differences of the observed and simulated daily mean precipitation accumulations and the three intensive periods (unit: mm d^{-1}) and the ratios of convective precipitation in the total precipitation

		GR-15-L14	GR-30-L14	GR-60-L14	GR-90-L14	GR-15-L23	GR-30-L23	GR-60-L23	GR-90-L23
Monthly precipitation	Difference	−1.76	−0.71	1.02	−1.96	−1.32	−1.33	−2.44	−3.18
	Ratio	74%	72%	66%	69%	87%	86%	86%	87%
Period I	Difference	3.03	11.41	19.65	11.49	2.67	10.70	5.80	7.27
	Ratio	82%	78%	65%	73%	91%	88%	87%	89%
Period II	Difference	−9.44	−14.08	−15.89	−18.08	−5.06	−12.03	−15.59	−16.79
	Ratio	81%	79%	72%	87%	89%	90%	93%	95%
Period III	Difference	−3.74	−4.08	−1.99	−7.85	−3.74	−5.64	−5.62	−10.01
	Ratio	71%	68%	67%	68%	86%	85%	85%	85%

3.2 Surface temperature

Continuous extreme precipitation processes caused lower local temperature in June 1999 over the Yangtze River Basin. The observed monthly surface temperature (Fig.5) shows that the high temperature

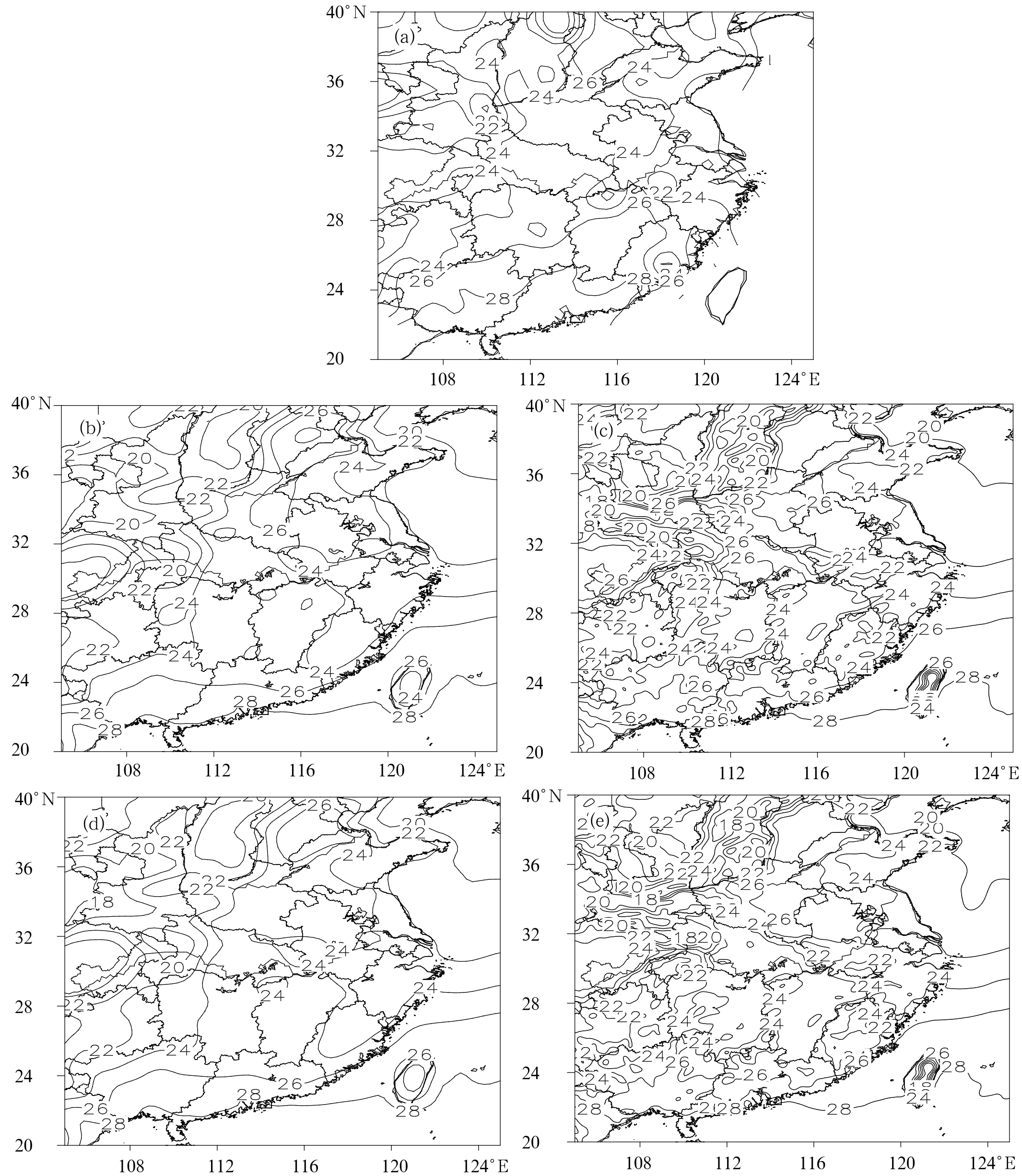

Fig.5. Monthly mean surface air temperature during June 1999 (unit: °C) for the observation (a), and simulations with the resolutions of 60 km and 14 levels (b), 60 km and 23 levels (c), 15 km and 14 levels (d), and 15 km and 23 levels (e).

is dominated in North and South China and the region with lower temperature of 24°C locates over the Yangtze River Basin. The simulations with different resolutions show major temperature distributions and underestimate surface temperature in South China. Experiments with a lower vertical resolution overestimate surface temperature in North China with an enlarged extent, and surface temperature is improved by increasing vertical levels over the region, such as enhanced results of the 60-km runs with 23 vertical levels than that with 14 levels. Similarly, the 15-km runs provide much better results in Sichuan and Shaanxi Provinces with a higher vertical resolution than the lower one. All runs at different horizontal scales characterize the general distribution with higher temperature over North and South China, and lower temperature over the Yangtze River Basin, such as the well simulated 24°C isopleths. The increase in horizontal resolution improves the temperature distribution reflecting terrain variation, e.g., the extent of the lower temperature of 22°C is not well depicted by the 60-km simulations, while such detailed features of the lower temperature is better represented by the 15-km runs.

3.3 Atmospheric circulation

Verification metrics of weather forecasts include the bias, root mean square error (RMSE), and correlation coefficient (COR).

The bias is defined as:

$$b_{\text{ias}} = \frac{\sum_i [\phi_i^{\text{M}} - \phi_i^{\text{O}}]}{N}.$$

The RMSE is defined as:

$$e_{\text{rms}} = \left(\frac{\sum_i (\phi_i^{\text{M}} - \phi_i^{\text{O}})^2}{N} \right)^{1/2}.$$

The COR is defined as:

$$R = \frac{\sum_i (\phi_i^{\text{M}} - \overline{\phi^{\text{M}}})(\phi_i^{\text{O}} - \overline{\phi^{\text{O}}})}{\left[\sum_i (\phi_i^{\text{M}} - \overline{\phi^{\text{M}}})^2 \sum_i (\phi_i^{\text{O}} - \overline{\phi^{\text{O}}})^2 \right]^{1/2}},$$

where ϕ_i^{M} is the model forecast, ϕ_i^{O} is the observation, and N is the number of the total events.

Figure 6 shows the difference of the simulated monthly mean sea level pressure (SLP) and the NCAR/NCEP reanalysis data. The simulated monthly mean SLP exhibits an overestimation over most regions in China, with a magnitude of about 1 hPa. Increasing vertical resolution shows few impacts on the simulation of monthly mean SLP, while increasing horizontal resolution improves the simulation and reduces the region having a difference of about 1 hPa. Table 3 clearly shows that the bias and RMSE decrease when the horizontal resolution changes from 90 to 30 km. However, the bias and RMSE increase at 15-km resolution. This increase perhaps results from the coarse resolution (1° × 1°) NCAR FNL data, which is unable to better represent the impacts of terrain and land surface processes on the change of SLP. At the low level of 700 hPa, the increase in vertical resolution reduces the bias of simulated geopotential height, temperature, and wind fields, and therefore improves the simulation of atmospheric variables at lower levels. By contrast, increasing horizontal resolution cannot reduce the bias and RMSE for atmospheric variables at lower levels. For the simulation of 500-hPa geopotential height, increasing vertical resolution always reduces the bias and RMSE, while the bias increases with increasing horizontal resolution. For the temperature simulation at the middle level of 500 hPa, the simulations with finer horizontal resolutions possess smaller biases with a high vertical resolution, while the biases increase with increasing horizontal resolution by using a lower vertical resolution.

Generally, when the vertical resolution increases, middle and low vertical levels in the model increase, which improve the model ability of simulating climate at lower atmospheric levels. The simulating synoptic characteristics at middle and high levels more depend on the atmospheric circulation, and are insensitive to the change of vertical resolution. The increase in horizontal resolution mainly improves the representation of climate impact factors, such as topography and land surface properties, and therefore better simulates synoptic characteristics on smaller scales. On the other hand, the biases may increase with increasing horizontal resolution. Therefore, the increase in horizontal resolution has not shown consistent improvements in simulations. For example, the simulation of precipitation, temperature, and atmospheric circulation with 15-km resolution does not consistently outperform the simulation with 30-km resolution. Several reasons are speculated for such inconsistency. First, the coarse resolution (1° × 1°) of the NCEP FNL dataset, which are used to drive the model, affects the simulation at high resolutions due to lack of detail mesoscale weather information. Second, the verification data of precipitation and temperature have coarser resolutions than the NCEP FNL data, and thereby reduce the effectiveness of verifying model results at high resolutions. Last, the selection of cumulus parameterization schemes with a

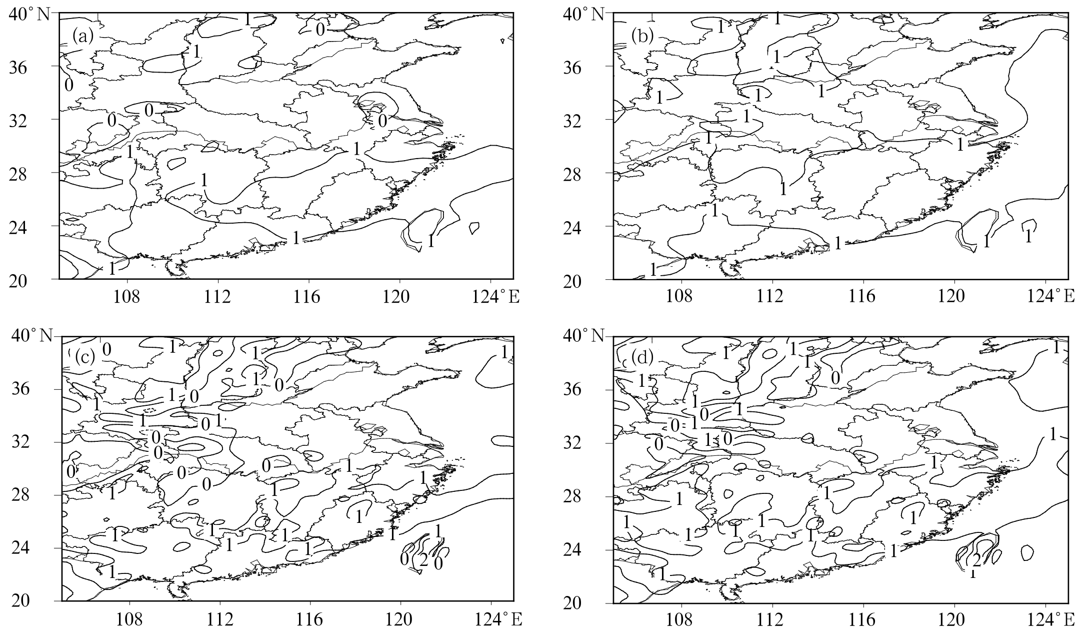

Fig.6. Differences of the observed and simulated mean sea level pressure (unit: hPa) at the resolutions of 60 km and 14 levels (a), 60 km and 23 levels (b), 30 km and 14 levels (c), and 30 km and 23 levels (d).

Table 3. Biases (BIASs), root mean square errors (RMSEs), and correlation coefficients (CORs) of sea level pressure (SLP); geopotential height (H) and temperature (T) at 500 and 700 hPa; and wind (U, V) at 200 and 700 hPa between observation and simulation (unit: SLP: hPa; temperature: °C; geopotential height: gpm; wind: m s^{-1})

	SLP			H500			T500			U200		
	BIAS	RMSE	COR	BIAS	RMSE	COR	BIAS	RMSE	COR	BIAS	RMSE	COR
GR-15-L14	0.76	0.96	0.91	−6.78	8.14	0.99	0.12	0.21	0.99	−0.80	1.58	0.99
GR-30-L14	0.61	0.78	0.94	−8.08	9.39	0.99	0.07	0.18	0.99	−0.81	1.66	0.99
GR-60-L14	0.69	0.81	0.95	−7.53	8.96	0.99	0.10	0.17	0.99	−0.87	1.88	0.99
GR-90-L14	0.88	0.98	0.94	−4.51	6.34	0.99	−0.05	0.17	0.99	−0.84	2.29	0.99
GR-15-L23	0.89	1.04	0.92	−6.91	7.98	0.99	−0.04	0.17	0.99	−0.43	1.09	0.99
GR-30-L23	0.80	0.92	0.94	−7.56	8.45	0.99	−0.10	0.19	0.99	−0.51	1.14	0.99
GR-60-L23	0.96	1.04	0.95	−6.74	7.75	0.99	−0.18	0.27	0.99	−0.39	1.51	0.99
GR-90-L23	1.09	1.17	0.93	−4.80	6.51	0.99	−0.21	0.28	0.99	−0.28	2.07	0.99
	H700			T700			U700			V700		
	BIAS	RMSE	COR	BIAS	RMSE	COR	BIAS	RMSE	COR	BIAS	RMSE	COR
GR-15-L14	−2.72	3.80	0.98	−0.28	0.51	0.97	0.02	1.01	0.94	0.35	0.96	0.90
GR-30-L14	−3.58	4.56	0.98	−0.35	0.55	0.97	0.06	1.07	0.93	0.44	1.02	0.90
GR-60-L14	−3.02	4.19	0.98	−0.38	0.58	0.97	0.10	1.01	0.94	0.39	1.07	0.88
GR-90-L14	−0.04	3.15	0.98	−0.27	0.48	0.97	0.07	1.05	0.93	0.13	0.99	0.87
GR-15-L23	−1.96	3.20	0.99	−0.30	0.46	0.98	−0.03	0.95	0.95	0.32	0.87	0.92
GR-30-L23	−2.49	3.29	0.99	−0.30	0.47	0.98	0.02	0.87	0.96	0.42	0.83	0.93
GR-60-L23	−1.47	2.62	0.99	−0.33	0.52	0.97	0.04	0.85	0.96	0.38	0.89	0.92
GR-90-L23	0.10	2.99	0.98	−0.27	0.47	0.97	0.03	0.99	0.94	0.10	0.94	0.88

fine resolution of 15 km needs further investigations.

3.4 Impacts on parameterization schemes

Previous experiments (Reynolds and Marsico, 1993) show that the simulation by different cumulus parameterization schemes varies and the increase of resolution affects the model results. In order to assess the impacts of different resolutions on cumulus parameterization schemes, both Kain-Fritsch (KF) and Grell (GR) schemes at varied resolutions are examined. The model results with 60- and 15-km resolutions show that the simulation by the KF scheme captures heavy precipitation over the lower Yangtze River Basin in June 1999 and improves the intensity comparable to the observations when the horizontal resolution increases (Fig.7). Similar to the Grell scheme, Table 4 shows monthly mean precipitation, the differences of the simulation and observations during the three intensive precipitation periods, and the ratios of the convective precipitation in the total precipitation by the KF scheme. The KF scheme also overestimates the first intensive period, and underestimates the second and third intensive precipitation periods. In contrast to the KF scheme, the Grell scheme shows increasing percentages with increasing vertical resolution. This indicates that the vertical resolution has different impacts on different cumulus parameterization schemes.

4. Conclusions and discussions

Impacts of changing horizontal and vertical resolution on intensive Meiyu events were analyzed through simulating extreme precipitation events by the NCAR MM5V3 over the Yangtze-Huaihe River Basin in June 1999. Several issues are generalized in the analyses as follows:

(1) The MM5V3 was able to simulate the distribution of extreme rainfall events for short-term climate change and daily variability. The model error of the precipitation simulation decreased by increasing horizontal resolution and the daily precipitation variability was more close to truth. Generally, the model ability to simulate extreme precipitation was improved.

Table 4. Same as Table 2, but for the Kain-Fritsch cumulus convective parameterization

		KF-15-L14	KF-30-L14	KF-60-L14	KF-90-L14	KF-15-L23	KF-30-L23	KF-60-L23	KF-90-L23
Monthly preciptiaiton	Difference	−1.35	−2.02	−1.53	−1.98	−1.75	−2.12	−4.13	−3.40
	Ratio	79%	79%	82%	84%	72%	75%	78%	79%
Period I	Difference	10.6	13.89	13.18	7.52	6.27	9.45	8.41	7.01
	Ratio	84%	87%	88%	90%	82%	83%	85%	86%
Period II	Difference	−3.13	−11.27	−14.42	−16.35	−6.47	−8.28	−12.99	−13.98
	Ratio	88%	81%	74%	81%	75%	74%	62%	72%
Period III	Difference	−9.39	−10.44	−7.07	−5.28	−7.18	−9.07	−13.38	−10.01
	Ratio	76%	76%	81%	83%	69%	71%	76%	78%

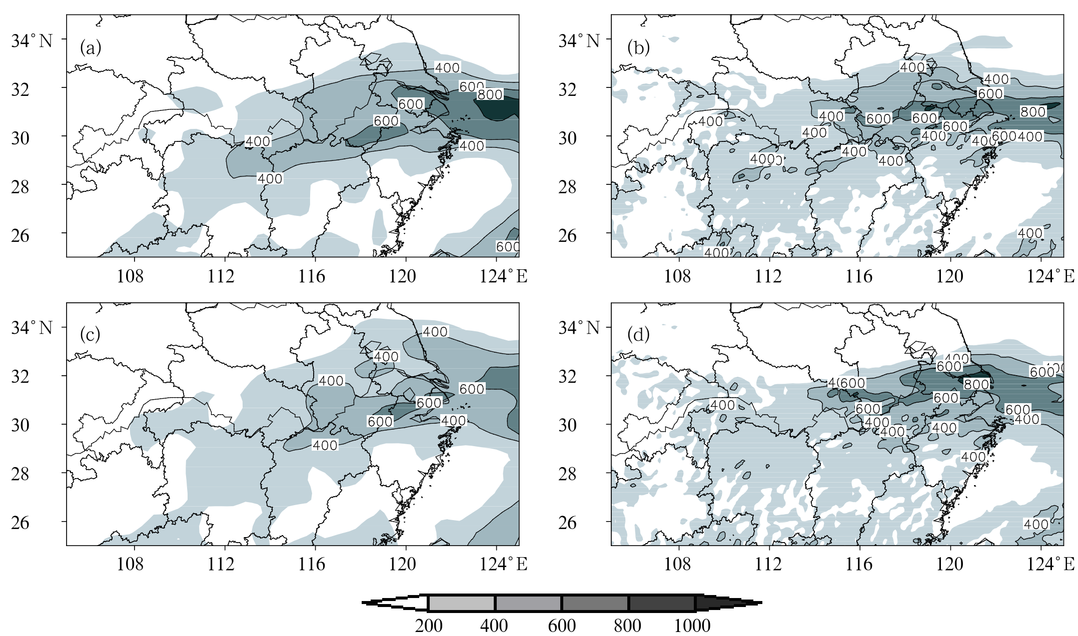

Fig.7. Simulated monthly precipitation over the middle and lower Yangtze River Basin in June 1999 with different resolutions by the Kain-Fristch cumulus convective parameterization (unit: mm).

With increasing horizontal resolution, the effects of orographic forcing and other local dynamics enhanced and localized extreme cells increased. The increase in vertical resolution showed consistent improvements in modeling extreme precipitation events with decreased errors.

(2) The models could well capture the characteristics of surface temperature, while surface temperature was lower than the observations in South China. Increasing both vertical and horizontal resolution improved the model simulation in surface temperature. Models with finer horizontal resolutions represented better topography, and thereby the change of local surface temperature was improved.

(3) In general, the simulation of surface sea level pressures was improved by increasing horizontal resolution, while the increase in vertical resolution could not advance the simulation. The increase in vertical resolution improved the physical processes and the atmospheric circulation at lower levels. The atmospheric circulation at middle and high levels was not sensitive to the change of vertical resolution.

(4) The distribution of extreme rainfall events by different cumulus parameterization schemes showed similar results. The ratios of convective precipitation varied with the change of horizontal resolution. The ratios by using the Grell scheme increased with increasing horizontal resolution, while the Kain-Fritsch scheme showed opposite changes.

In summary, increasing both horizontal and vertical resolution can improve the model ability to simulate extreme precipitation events as well as the atmospheric circulation at low levels. However, detailed analyses on the impacts of high resolution are associated with higher-resolution observation data. For this reason, local intensive weather forecasts by orographic forcing have not been examined, considering the limitation of available observation datasets. Due to limited computing resources, only one short-term extreme event was analyzed in detail. More extreme events need to be investigated in the future, in order to better understand the effects of the resolution on short-term climate change.

REFERENCES

Chen Fei and Jimy Dudhia, 2001a: Coupling an advanced land surface-hydrology model with the Penn State-NCAR MM5 modeling system. Part I: Model implementation and sensitivity. *Mon. Wea. Rev.*, **129**, 569-585.

Chen Fei and Jimy Dudhia, 2001b: Coupling an advanced land surface-hydrology model with the Penn State-NCAR MM5 modeling system. Part II: Preliminary model validation. *Mon. Wea. Rev.*, **129**, 587-604.

Christensen, O. B., J. H. Christensen, B. Machenhauer, and M. Botzet, 1998: Very high-resolution regional climate simulations over Scandinavia-Present climate. *J. Climate*, **11**, 3204-3229.

Colle, B. A., C. F. Mass, and K. J. Westrick, 2000: MM5 precipitation verification over the Northwest Pacific during the 1997-1999 cool seasons. *Wea. Forecasting*, **15**, 730-744.

Denis, B., R. Laprise, J. Cote, and D. Caya, 2002: Downscaling ability of one-way nested regional climate models: The big-brother experiment. *Climate Dyn.*, **18**, 627-646.

Gao Xuejie, Zhao Zongci, Ding Yihui, et al., 2003: Climate change due to greenhouse effects in China as simulated by a regional climate model. Part II : Climate change. *Acta Meteorologica Sinica*, **61**(1), 29-38. (in Chinese)

Giorgi, F., M. Arinucci, and G. T. Bates, 1993a: Development of a second-generation regional climate model (RegCM2). Part I: Boundary-layer and radiative transfer processes. *Mon. Wea. Rev.*, **121**, 2794-2813.

Giorgi, F., M. Arinucci, and G. T. Bates, 1993b: Development of a second-generation regional climate model (RegCM2). Part II: Convective processes and assimilation of lateral boundary conditions. *Mon. Wea. Rev.*, **121**, 2814-2832.

Giorgi, F., and M. R. Marinuci, 1996: An investigation of the sensitivity of simulated precipitation to model resolution and its implications for climate studies. *Mon. Wea. Rev.*, **124**, 148-166.

Giorgi, F., and Coauthors, 2001: Regional climate information-evaluation and projections. *Climate Change 2001: The Scientific Basis*. Houghton, J. T. et al., Ed., Cambridge University Press, 583-638.

Kalnay, E., S. J. Lord, and R. D. McPherson, 1998:

Maturity of operational numerical weather prediction: Medium range. *Bull. Amer. Meteor. Soc.*, **79**, 2753-2769.

Leung, L. R., L. O. Mearns, F. Giorgi, and R. Wilby, 2003: Workshop on regional climate research: Needs and opportunities. *Bull. Amer. Meteor. Soc.*, **84**, 89-95.

Leung, L. R., and Qian Y., 2003: The sensitivity of precipitation and snowpack simulations to model resolution via nesting in regions of complex terrain. *J. Hydrometeor.*, **4**(6), 1025-1043.

Leung, L. R., Qian Y., and Bian X., 2003a: Hydroclimate of the western United States based on observations and regional climate simulation of 1981-2000. Part I: Seasonal statistics. *J. Climate*, **16**, 1892-1911.

Leung, L. R., Qian Y., Bian X., and A. Hunt, 2003b: Hydroclimate of the western United States based on observations and regional climate simulation of 1981-2000. Part II: Mesoscale ENSO anomalies. *J. Climate*, **16**, 1912-1928.

Liang, X-Z, K. E. Kunkel, and A. N. Samel, 2001: Development of a regional climate model for US midwest applications. Part I: Sensitivity to buffer zone treatment. *J. Climate*, **14**, 4363-4378.

Liu Dong, 2003: Performance verification of mesoscale model MM5V3 to regional climate simulation, *Plateau Meteorology*, **22**(1), 71-77. (in Chinese)

Reynolds, R. W., and D. C. Marsico, 1993: An improved real-time global sea surface temperature analysis. *J. Climate*, **6**, 114-119.

Su Bingkai, Tang Jianping, Zhong Zhong, et al., 2002: A research on high performance simulator for disaster weather and climate. *J. Nanjing University (Natural Sciences)*, **38**(3), 366-375. (in Chinese)

Tang Jianping, Su Bingkai, and Zhao Ming, 2003: Combinatorial optimization using MM5V3's various parameterizations in different physical processes: Regional climate simulation in East Asia. *J. Nanjing University (Natural Sciences)*, **39**(6), 754-769. (in Chinese)

Wang Y., L. R. Leung, J. L. McCregor, et al., 2004: Regional climate modeling: Progress, challenges, and prospects. *J. Meteor. Soc. Japan*, **82**, 1599-1628.

Zhao Zongci and Luo Yong, 1998: Advances in regional climate modeling since 1990. *Acta Meteorologica Sinica*, **56**(2), 225-246. (in Chinese)

Zhao Zongci and Luo Yong, 1999: Investigations of application for the regional climate model over East Asia. *Chinese Journal of Atmospheric Sciences*, **23**(5), 522-532. (in Chinese)